

Solubility of Corosolic Acid in Supercritical Carbon Dioxide and Its Representation Using Density-Based Correlations

Andri C. Kumoro*

Department of Chemical Engineering, Faculty of Engineering, Diponegoro University Prof. H. Soedarto, SH Road, Tembalang-Semarang 50239, Indonesia

ABSTRACT: The solid solubilities of $2\alpha,3\beta$ -dihydroxyurs-12-en-28-oic acid (corosolic acid) in supercritical carbon dioxide (SC-CO₂) have been measured using a dynamic method at (308.15, 313.15, 323.15, and 333.15) K over a pressure range of (8 to 30) MPa. Prior to solubility measurements, the accuracy of the experimental apparatus was examined by measuring solubilities of squalene in SC-CO₂ and comparing them with literature. The corosolic acid solubilities ranged from a corosolic acid mole fraction of $3.28 \cdot 10^{-11}$ at 333.15 K and 8 MPa to $7.43 \cdot 10^{-2}$ at 333.15 K and 30 MPa. The del Valle and Aguilera and Méndez-Santiago and Teja (density-based) models were used to correlate the experimental data. The calculated solubilities showed good agreement with the experimental data in the temperature and pressure ranges studied.

INTRODUCTION

Diabetes mellitus is one of the world's major health problems. In the developed countries, diabetes mellitus patients may have proper treatments, such as controlled low sugar diet and administration of insulin and/or hypoglycaemic agents. Unfortunately, patients in the developing countries may not be able to afford these methods due to their socio-economic conditions.¹ This fact has prompted to the high prevalence of noncompliance observed in minority, disadvantaged communities in the developed countries, and rural folks in the developing countries.² In addition, medical centers are not always available within the reach of these population groups, and rural folks prefer to seek traditional medications rather than the modern ones. In Asia and South America, the development and use of inexpensive and easily accessible phytomedicines from plants of the genus *Syzygium* in the treatment of diabetes mellitus is encouraged to overcome these problems.³

Corosolic acid ($2\alpha,3\beta$ -dihydroxyurs-12-en-28-oic acid, IUPAC 1S,2R,4aS,6aR,6aS,6bR,10R,11R,12aR,14bR)-10,11-dihydroxy-1,2,6a,6b,9,9,12a-heptamethyl-2,3,4,5,6,6a,7,8,8a,10,11,12,13,14b-tetradecahydro-1H-picene-4a-carboxylic acid, CAS Registry No. 4547-24-4, Figure 1) is one of the secondary metabolites contained in the leaf of *Syzygium cumini*, which has antidiabetic activity.^{4,5} Miura and coworkers⁶ reported an acute hypoglycemic effect of corosolic acid, which was shown by an increase in GLUT4 translocation in mouse muscle. In addition, they also found that corosolic acid promotes glucose metabolism by reducing insulin resistance. The action of insulin is mediated by tyrosine phosphorylation and initiated by the binding of insulin to the insulin receptor. Corosolic acid may act as an insulin sensitizer, enhancing insulin receptor B phosphorylation indirectly by inhibiting certain nonreceptor protein tyrosine phosphatases.⁷ Latter, Fukushima et al.⁵ have discovered corosolic acid ability to reduce post challenge plasma glucose levels in humans. Another study reported that corosolic acid inhibited gluconeogenesis by increasing the production of the gluconeogenic intermediate fructose-2,6-bisphosphate in isolated

hepatocytes.^{8,9} Bhat et al.¹⁰ have demonstrated various levels antidiabetic activity of corosolic acid obtained from aqueous and organic solvent extraction of *S. cumini* plant leaf. No antidiabetic activity was shown by aqueous and methanol extracts, while chloroform extract showed good antidiabetic activity. In addition, it has also been reported that in general, secondary metabolites are highly unstable depending on factors like temperature, light, oxygen, and solvent used in the extraction.^{11–14}

Supercritical fluid extraction (SFE) has shown its superiority over conventional solvent extraction techniques. The absence of both light and air during the extraction process along with relatively mild operating temperatures can reduce the tendency of degradations, while the use of CO₂ as solvent allows working in an environmentally clean media. The possibility of adjusting the supercritical solvent power based on its density is the key factor in the extraction process. Then, information of solubility of corosolic acid in the supercritical condition is necessary for the analyses and optimization of corosolic acid extraction and purification units.

This article reports experimental measurements of corosolic acid solubilities in supercritical CO₂, which, to the best of the author knowledge, has not been reported in the literature until present. Four density-based correlations on the solubility of solute in supercritical CO₂ were used in this work to represent the solubility data.

EXPERIMENTAL METHODS

Materials. Corosolic acid (C₃₀H₄₀O₄, purity > 0.96 mass fraction) was purchased from Dalian GreenPeak Biotech Co. Ltd. China and used as received without any further treatments. Deionized water, squalene (Fluka Chemie, high-performance liquid chromatography (HPLC) grade, purity ≥ 0.97 mass

Received: November 16, 2010

Accepted: February 8, 2011

Published: February 25, 2011

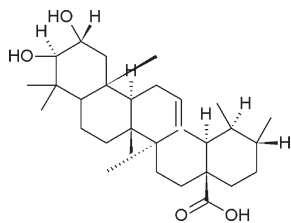


Figure 1. Structure of the corosolic acid molecule.

fraction) and anhydrous methanol (HPLC grade, purity ≥ 0.998 mass fraction) were purchased from Sigma-Aldrich Pte. Ltd. Singapore and stored at 291.15 K. Orthophosphoric acid (HPLC grade, purity ≥ 0.998 mass fraction) was purchased from Merck, Germany. Carbon dioxide (0.99 mass fraction) was provided in liquid form in cylinders equipped with a diptube, and it was further purified by passing it through a $2\ \mu\text{m}$ filter (PT. Aneka Gas, Indonesia).

Procedure. The solubility of corosolic acid in supercritical carbon dioxide (SC- CO_2) was determined using a dynamic method. This method is based on the assumption that the solute–solvent system reaches equilibrium as the solvent flows over the solute.¹⁵ Preliminary solubility measurements were carried out by delivering carbon dioxide (liquid based) into the equilibrium cell at flow rates ranging from $(6.67 \cdot 10^{-9}$ to $3.33 \cdot 10^{-8})\ \text{m}^3 \cdot \text{s}^{-1}$ for about 4 h. Variation of the flow rate within this range was found to have no effect on the observed solubilities, thereby confirming that equilibrium between the solid phase and the fluid phase was achieved at these flow rates and that there were no mass-transfer limitations. Hence, the supercritical carbon dioxide solvent leaving the extraction vessel was saturated with the solute and equilibrium between the solid and the supercritical phase was achieved. The solubility of corosolic acid in SC- CO_2 was measured using the same apparatus that was described in the literature¹⁶ and explained briefly here (see Figure 2). The main apparatus was a $1.6 \cdot 10^{-5}\ \text{m}^3$ high-pressure stainless steel equilibrium cell (H) (10 mm inner diameter \times 210 mm length) immersed in a water bath (A) controlled by an electrical heater (D) (model DC10, Thermo Haake) to within $\pm 0.1\ \text{K}$ uncertainty. The system pressure was indicated by a pressure transducer (G) (model PDCR 961, Druck). Its uncertainty was $\pm 0.01\ \text{MPa}$ in the pressure range of (8 to 30) MPa, while an HPLC pump (C) (model LC-6A, Shimadzu Co.) was used to compress the liquid CO_2 and to deliver it at a constant volumetric flow rate of $1.67 \cdot 10^{-8}\ \text{m}^3 \cdot \text{s}^{-1}$. The CO_2 was depressurized to atmospheric by a back pressure regulator/BPR (J) (model BP 1580-81, JASCO) with uncertainty of $\pm 0.01\ \text{MPa}$ and the amount of CO_2 consumed was quantified using a wet gas meter (L) (model DM 3A, Alaxander Wright & Co.) within the time of measurement to calculate the expanded gas flow rate ($\pm 1.0 \cdot 10^{-10}\ \text{m}^3 \cdot \text{s}^{-1}$). The solute collected was gravimetrically determined using an analytical balance (model AG 204, Mettler Toledo) with an accuracy of $\pm 0.0001\ \text{g}$. However, when the amount of corosolic acid was not possible to be measured using the analytical balance, then the HPLC analysis was applied to quantify the exact amount of corosolic acid in the vial. It was done by washing the vial using a solution, which was a mixture of methanol and aqueous orthophosphoric acid. The concentrations of methanol and orthophosphoric acid in the solution were $27.39\ \text{mol} \cdot \text{kg}^{-1}$ and $1.25 \cdot 10^{-2}\ \text{mol} \cdot \text{kg}^{-1}$, respectively. The collected washing liquid was then subjected to corosolic acid analysis using the HPLC method.¹⁶

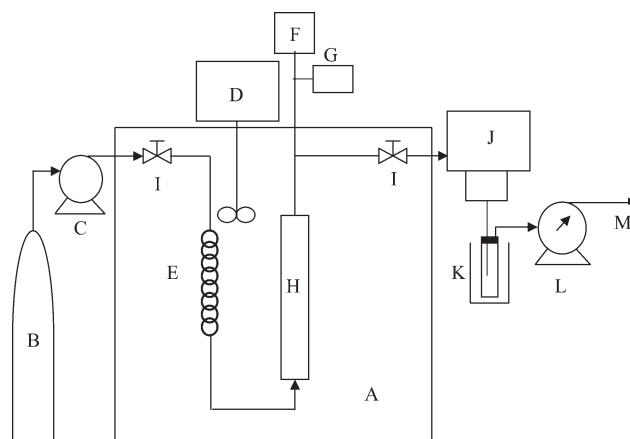


Figure 2. Schematic diagram of isothermal solubility measurement apparatus. A, constant temperature water bath; B, CO_2 tank; C, CO_2 pump; D, controlled electric heater with water circulation pump; E, heating coil; F, temperature indicator; G, pressure transducer; H, equilibrium cell; I, micrometer valve; J, backpressure regulator; K, cold trap; L, wet gas meter, and M, vent.

This method was valid for corosolic acid concentration ranged from $(4.5$ to $400)\ \text{g} \cdot \text{m}^{-3}$. Prior to solubility experiments, the equilibrium cell was washed with ethanol, dried in an electric oven at 373.15 K for one hour, and cooled in a desiccator. On the other hand, the tube lines, fittings, and connections were cleaned up by flushing liquid CO_2 at $3.33 \cdot 10^{-8}\ \text{m}^3 \cdot \text{s}^{-1}$ for about 900 s to totally remove dirt and solute.

A total of 10 g of corosolic acid was charged into a stainless-steel equilibrium cell by arranging it into alternative layers of about 500 mg and glass beads (30 to 60) mesh, with glass wool at either end. The function of the packing was to improve corosolic acid–SC- CO_2 contact, reduce channeling of the SC- CO_2 , and prevent corosolic acid entrainment.¹⁷ The equilibrium cell was heated to the prescribed temperature value by immersing it in a controlled temperature water bath. The liquid CO_2 was pressurized and delivered at a flow rate of $1.67 \cdot 10^{-8}\ \text{m}^3 \cdot \text{s}^{-1}$ using a reciprocating HPLC pump to pass through a heating coil immersed in the water bath and enabled CO_2 to reach the desired temperature before entering the equilibrium cell at a constant pressure. The system pressure was maintained by a back-pressure regulator, and the value was indicated by a test gauge. The saturated SC- CO_2 was then depressurized by the BPR to atmospheric, and the dissolved compound was trapped and collected in a vial cooled in a table salt solution of 277.15 K after exiting from the BPR. To prevent precipitation of the solute between BPR and the trap, short tape heater tubing and the BPR-heater-jacket temperature of 333.15 K were used. The weight loss of the cell was also compared with the weight of the collected solute to ensure at least 96 % of trapping efficiency during solubility measurements. The solubility was defined as the mole fraction of the solutes in the expanded CO_2 . The corosolic acid solubility experiments were performed at (308.15, 313.15, 323.15, and 333.15) K and at pressures ranging from (8 to 30) MPa. The reproducibility of the measurements was confirmed by making triplicates of each measurement to obtain reliable solubility values, and an average value was given. The estimated uncertainty of the solubility values based on error analysis and repeated observations was within 2 %. To verify the accuracy of the solubility measurements and the method employed, the solubility of squalene in SC- CO_2 had been measured and compared with the literature values.

RESULTS AND DISCUSSION

Apparatus Validation. It was imperative for the author to ensure that the experimental technique was adequate. However, no literature values for corosolic acid solubility in SC-CO₂ could be found. Fortunately, the solubility of a close compound in the same homologous series (i.e., squalene) in SC-CO₂ is available in the literature, which could have served as an indirect way to validate the results. Experiments were performed at (323.15 and 333.15) K and at pressures of (10 to 27.5) MPa. The procedure was identical to that used for the corosolic acid experiments, including equilibrium determination and runs in triplicate. Table 1 presents and compares the experimental solubility of pure squalene in SC-CO₂ (grams of squalene per kilograms of CO₂) at pressures of (10 to 27.5) MPa obtained from this work and those reported by Catchpole and von Kamp.¹⁸ The experimental results show good agreement with the literature, where the solubility values obtained in this work are almost equal with those reported in the literature. These results validate the experimental method used in this study.

Solubility Data. The solubility values of corosolic acid in pure SC-CO₂ obtained in this work are summarized in Table 2 and plotted in Figure 3. Most of the CO₂ density values were obtained from the National Institute of Standards and Technology (NIST) fluid property database.¹⁹ When the CO₂ density value was not readily available, its value was then predicted using REFPROP program available in the NIST database. In general, as pressure increased at constant temperature, the solubility of corosolic acid in SC-CO₂ also increased. This was expected because an increase in SC-CO₂ pressure at a constant temperature results in increasing its density and thereby its solvent strength (ability of a solvent to dissolve solute).²⁰ The increases of CO₂ density with pressure causing a decrease of the intermolecular distances which increases the solute–solvent interaction. Therefore, at lower pressures, corosolic acid solubility in SC-CO₂ at 333.15 K is the lowest. In addition, temperature also affects the solute vapor pressure, the solvent density, and the intermolecular interactions in the fluid phase. At a constant pressure, an increase in temperature will reduce the ability of SC-CO₂ to dissolve corosolic acid due to the reduction of SC-CO₂ density.²⁰ On the other hand, an increase in temperature will increase the vapor pressure of corosolic acid, which leads to an increase in the dissolution of corosolic acid in SC-CO₂. Therefore, it is not surprising that a crossover pressure occurs between at about 20.0 MPa. Such retrograde behavior has also been

Table 1. Solubility of Squalene in CO₂

<i>p</i> /MPa	323.15 K/g·kg ⁻¹		333.15 K/g·kg ⁻¹	
	Catchpole and von Kamp ¹⁷	this work	Catchpole and von Kamp ¹⁷	this work
10.0	0.27	0.26		
12.0		4.42		
15.0	10.63	10.65		3.12
17.5	17.38			
18.0		18.91		12.60
20.0	23.84	23.79		19.01
22.5	30.12		27.05	
25.0			34.65	34.73
27.5			43.00	

Table 2. Mole Fraction Solubility (*x*₂) of Corosolic Acid in Carbon Dioxide in the Temperature Range (308.15 to 333.15) K

<i>p</i> /MPa		10 ² ·(<i>x</i> ₂)
	308.15 K	
8.00		6.36·10 ⁻⁵
10.00		1.86·10 ⁻¹
12.00		2.06
15.00		3.42
16.00		3.71
18.00		4.17
20.00		4.54
25.00		4.85
28.00		4.92
30.00		4.95
	313.15 K	
8.00		1.79·10 ⁻⁴
10.00		1.13·10 ⁻¹
12.00		1.08
15.00		3.00
16.00		3.47
18.00		4.07
20.00		4.56
25.00		5.24
28.00		5.41
30.00		5.48
	323.15 K	
8.00		4.18·10 ⁻⁸
10.00		9.37·10 ⁻⁵
12.00		1.91·10 ⁻¹
15.00		1.22
16.00		1.98
18.00		3.47
20.00		4.54
25.00		5.91
28.00		6.31
30.00		6.51
	333.15 K	
8.00		3.28·10 ⁻⁹
10.00		7.58·10 ⁻⁷
12.00		5.64·10 ⁻⁴
15.00		1.69·10 ⁻¹
16.00		4.08·10 ⁻¹
18.00		1.54
20.00		4.55
25.00		6.30
28.00		7.10
30.00		7.43

reported before for different organic compounds.^{21,22} The crossover phenomena could be attributed to the competitions between solute's vapor pressure and solvent's density, whose temperature dependences are in opposite directions. At the crossover point, the effects of solute vapor pressure and solvent density on solid solubility balance each other. From the crossover

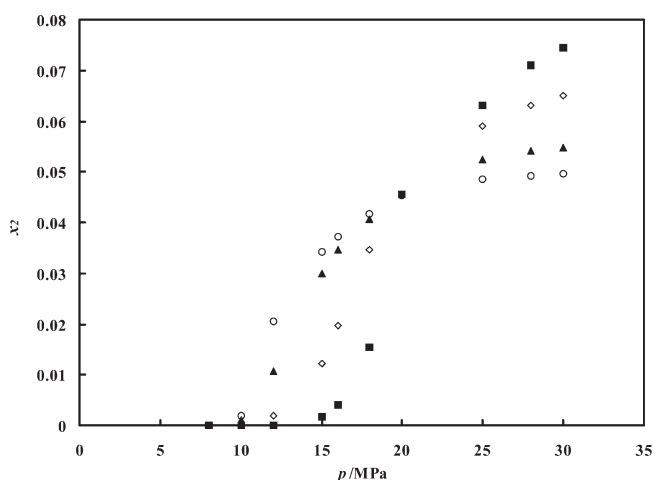


Figure 3. Mole fraction solubility (x_2) of corosolic acid in supercritical carbon dioxide at elevated pressure: \circ , 308.15 K; \blacktriangle , 313.15 K; \diamond , 323.15 K; \blacksquare , 333.15 K.

pressure point and upward, the solubilities of corosolic acid in SC- CO_2 at 333.15 K were higher than at any other temperatures in this study. This phenomenon indicated that the vapor pressure of corosolic acid began to have a dominant effect on solubility.^{17,23}

Modeling. There are two most common approaches in the modeling of solubility of solute in supercritical fluid, namely, the so-called semiempirical methods and the equation-of-state (EOS) methods. Considering the calculation simplicity and further applications, some semiempirical correlations were tested in this work.

By assuming chemical association equilibrium between the solute and the compressed gas, Chrastil developed a theory based on the mass action law applied to the formation of a solvate complex between a solute molecule and a number of supercritical fluid (SCF) solvent molecules.²⁴ It should be noted that the associated solvate complex assumption is quite close to the cluster conception accepted by the community.²⁵ Based on the facts that k is a function of density²⁶ and that the solubility is a function of temperature, del Valle and Aguilera proposed a model to help compensate for the change in the heat of vaporization with temperature in the original Chrastil model. They also recommended the equation to be used for a temperature range from (293 to 353) K and for pressure varying from (15 to 88) MPa.²⁷

This idea leads to the following equation for the solubility of component 2 (solid or liquid) in component 1 (SCF):

$$\ln S = k \ln \rho_f + A + \frac{B}{T} + \frac{C}{T^2} \quad (1)$$

$$S = \frac{\rho_f MW_2 x_2}{MW_1 (1 - x_2)} \quad (2)$$

In eq 1, S is the concentration of solute in the supercritical fluid ($\text{kg} \cdot \text{m}^{-3}$); ρ_f is the density of the supercritical fluid ($\text{kg} \cdot \text{m}^{-3}$); k is an association number; A is a function of the molecular weights of the solute and supercritical fluid; B and C are parameters related to the heat of solvation and heat of vaporization; and T is temperature (K). In eq 2, MW_1 , MW_2 , and x_2 are the molecular weight of SCF and solute and mole fraction solubility of solute in SCF, respectively.

Table 3. Optimized Parameters of the DVA and MST Equations for Corosolic Acid Solubility in Supercritical Carbon Dioxide

model	parameters	AARD, %
DVA	$A = -35.6134$	17.2
	$B = -0.3234$	
	$C = -0.8689$	
	$k = 6.1584$	
MST	$D = 11957.5581$	14.7
	$F = 2.7811$	

The measured solubility values are usually much greater than predicted using ideal gas theory. The extent to which pressure enhances the solubility of the solid in the gas is shown by an examination of the enhancement factors E of the solutes, where:

$$E = \frac{x_2 P}{P_2^{\text{sat}}} \quad (3)$$

and P is the total system pressure, and P_2^{sat} is the saturation (or, for solid solutes, sublimation) pressure of the pure solute. The vapor pressure of the solid, necessary to calculate the enhancement factor using eq 3, can be predicted according to the method proposed by Grain.²⁸ On the basis of the dilute solutions theory, Méndez-Santiago and Teja²⁹ proposed the other model to fit the corosolic solubility data, which started with Henry's constant of the dilute solution and demonstrated that the solubility plotted as $T \ln E$ against the density of the solvent would yield a single line. They also concluded that the fact that all isotherms collapse to a single line is thus a powerful tool to determine the self-consistency of experimental data. The model can be written as

$$T \ln E = D + F \rho_f \quad (4)$$

where D and F are the equation parameters. Both D and F are independent of temperature.

In the calculations, the objective function used is the average absolute relative deviation (AARD) between the calculated and experimental solubility:

$$\text{AARD} = \frac{1}{N} \sum_1^N \left(\frac{|x_{2\text{calc}} - x_{2\text{exp}}|}{x_{2\text{exp}}} \right) \quad (5)$$

where N is the number of experimental data points. The $x_{2\text{exp}}$ and $x_{2\text{calc}}$ are experimental and calculated solubility values, respectively.

The parameters A , B , C , and k to facilitate the incorporation of effect of temperature and solvent density of the del Valle and Aguilera (DVA) equation together with the AARD between experimental and calculated solubility are presented in Table 3. The plots of the experimental data and the solubility isotherms calculated with the DVA model are presented in Figure 4, where the quality of the correlations can be visually evaluated. It is obvious in Figure 4 and Table 3 that the model still produced reasonable solubility estimation compared with the experimental data, where an AARD of 17.2 % was obtained. The correlation improves largely when the correlation parameters were evaluated without taking into account the low solubility data since solubilities are often in the same order of magnitude, as this equation does not require the thermodynamic properties of the pure component which is not always available in the literature.

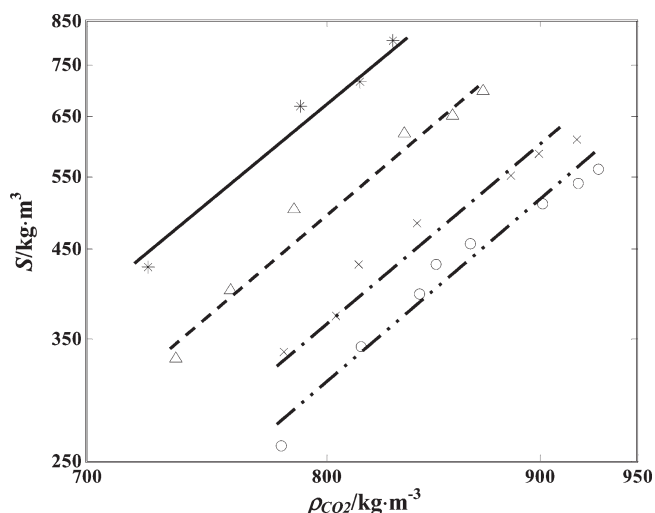


Figure 4. Solubility (S) of corosolic acid in carbon dioxide as a function of carbon dioxide density and temperature: \circ , 308.15 K; \times , 313.15 K; \triangle , 323.15 K; $*$, 333.15 K. The lines are the best fit of the experimental data calculated with DVA equation; $-\cdot-$, 308.15 K; $- \cdot -$, 313.15 K; $- \cdot -$, 323.15 K; $-\cdot-$, 333.15 K.

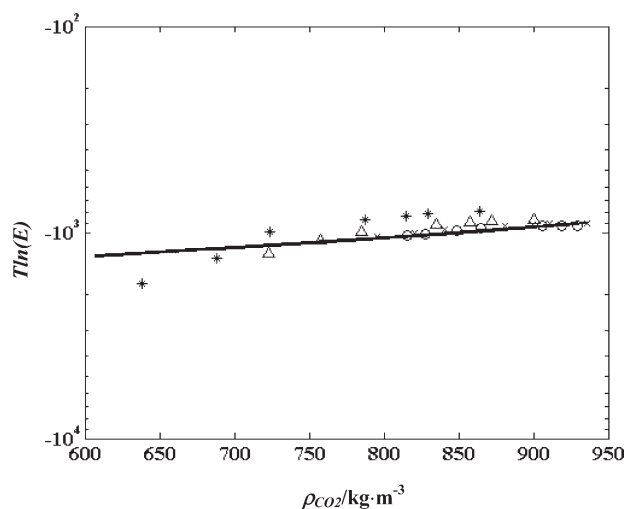


Figure 5. Enhancement factor (E) of corosolic acid solubility in supercritical carbon dioxide as a function of carbon dioxide density: \circ , 308.15 K; \times , 313.15 K; \triangle , 323.15 K; $*$, 333.15 K; $—$ is the best fit line of the experimental data calculated with MST equation.

When vapor pressure data is available, the original version of the MST model is very useful for data correlation because of its simplicity and good fitting results. With the purpose of regression analysis of the MST equation, P , ρ , and T were expressed in MPa, $\text{kg} \cdot \text{m}^{-3}$, and K, respectively. The values for D and F obtained via multilinear regression are reported in Table 3. Although MST equation uses only two adjustable parameters, it results in better solubility calculations than DVA equation by generating an AARD as low as 14.7 %. Figure 5 shows that the data points for the four isotherms follow a single trend, indicating good consistency of the data over the range of temperatures tested. It may be observed that the model reproduces much better calculation when the parameters are obtained without including the solubilities obtained at pressures in the vicinity of the critical point of carbon dioxide.

CONCLUSIONS

The solubility of corosolic acid in supercritical carbon dioxide has been measured experimentally. The solubility varied from a mole fraction of $3.28 \cdot 10^{-11}$ at 333.15 K and 8.0 MPa to $7.43 \cdot 10^{-2}$ at 333.15 K and 30.0 MPa. In general, the solubility of corosolic acid increased with increasing pressure at constant temperature. Overall, the solubility of corosolic acid in supercritical carbon dioxide increased with pressure at a constant temperature. Retrograde behavior of this system was indicated by a crossover pressure at 20.0 MPa. The solubility data were modeled with two density based semiempirical equations. The MST equation performed its superiority over the DVA models in term of accuracy with an AARD of 14.7 %, and its also successfully tested the consistency of the data. To the author's knowledge, this is the first reported data of corosolic acid solubility in SC-CO_2 .

AUTHOR INFORMATION

Corresponding Author

*Tel.: +62-24-7460058, Fax: +62-24-76480675, e-mail: c.k.andrew@undip.ac.id.

Funding Sources

The author would like to express their gratitude to the Directorate General of Higher Education, Ministry of National Education The Republic of Indonesia for its financial support through Hibah Kompetensi/Competence Research Grant 2010.

REFERENCES

- (1) Ducorps, M.; Ndong, W.; Jupkwo, B.; Belmejdoub, G.; Thiolet, C.; Mayaudon, H.; Bauduceau, B. Diabetes in Cameroon. Classification difficulties in Africa. *Med. Trop.* **1996**, *56*, 264–270.
- (2) Dyer, P. H.; Lloyd, C. E.; Lancashire, R. J.; Bain, S. C.; Barnett, A. H. Factors associated with clinic non-attendance in adults with type-1 diabetes mellitus. *Diabetic Med.* **1998**, *15*, 339–343.
- (3) Teixeira, C. C.; Pinto, L. P.; Kessler, F. H.; Knijnik, L.; Pinto, C. P.; Gastaldo, G. J.; Fuchs, F. D. The effect of *Syzygium cumini* (L.) skeels on post-prandial blood glucose levels in non-diabetic rats and rats with streptozotocin-induced diabetes mellitus. *J. Ethnopharmacol.* **1997**, *56*, 209–213.
- (4) Wen, X.; Sun, H.; Liu, J.; Wu, G.; Zhang, L.; Wu, X.; Ni, P. Pentacyclic triterpenes. Part 1: the first examples of naturally occurring pentacyclic triterpenes as a new class of inhibitors of glycogen phosphorylases. *Bioorg. Med. Chem. Lett.* **2005**, *15*, 4944–4948.
- (5) Fukushima, M.; Matsuyama, F.; Ueda, N.; Egawa, K.; Takemoto, J.; Kajimoto, Y.; Yonaha, N.; Miura, T.; Kaneko, T.; Nishi, Y.; Mitsui, R.; Fujita, Y.; Yamada, Y.; Seino, Y. Effect of corosolic acid on postchallenge plasma glucose levels. *Diabetes Res. Clin. Pract.* **2006**, *73*, 174–177.
- (6) Miura, T.; Ueda, N.; Yamada, K.; Fukushima, M.; Ishida, T.; Kaneko, T.; Matsuyama, F.; Seino, Y. Antidiabetic effects of corosolic acid in KKAY diabetic mice. *Biol. Pharm. Bull.* **2006**, *29*, 585–587.
- (7) Shi, L.; Zhang, W.; Zhou, Y. Y.; Zhang, Y. N.; Li, J. Y.; Hu, L. H.; Li, J. Corosolic acid stimulates glucose uptake via enhancing insulin receptor phosphorylation. *Eur. J. Pharmacol.* **2008**, *584* (1), 21–29.
- (8) Klein, G.; Kim, J.; Himmeldirk, K.; Cao, Y.; Chen, X. Antidiabetes and anti-obesity activity of *Lagerstroemia speciosa*. *Evidence-Based Complement. Alternat. Med.* **2007**, *4* (4), 401–407.
- (9) Yamada, K.; Hosokawa, M.; Fujimoto, S.; Fujiwara, H.; Fujita, Y.; Harada, N.; Yamada, C.; Fukushima, N.; Ueda, N.; Kaneko, T.; Matsuyama, F.; Yamada, Y.; Seino, Y.; Inagaki, N. Effect of corosolic acid on gluconeogenesis in rat liver. *Diabetes Res. Clin. Pract.* **2008**, *80*, 48–55.
- (10) Bhat, M.; Zinjarde, S. S.; Bhargava, S. Y.; Kumar, A. R.; Joshi, B. N. Antidiabetic Indian Plants: a Good Source of Potent Amylase

Inhibitors. *Evidence-Based Complement. Alternat. Med.* **2008**, 1–6; doi:10.1093/ecam/nen040

(11) Schwarz, K.; Ternes, W. Antioxidative constituents of *Rosmarinus officinalis* and *Salvia officinalis* II. Isolation of carnosic acid and formation of other phenolics diterpenes. *Z. Lebensm. Unters. Forsch.* **1992**, 195, 99–103.

(12) Schwarz, K.; Ternes, W.; Schmauderer, E. Antioxidative constituents of *Rosmarinus officinalis* and *Salvia officinalis* III. Stability of phenolic diterpenes of rosemary extracts under thermal stress as required for technological processes. *Z. Lebensm. Unters. For.* **1992**, 195, 104–107.

(13) Cuvelier, M. E.; Berset, C.; Richard, H. Antioxidant constituents in sage (*Salvia officinalis*). *J. Agric. Food Chem.* **1994**, 42, 665–669.

(14) Okamura, N.; Fujimoto, Y.; Kuwabara, S.; Yagi, A. High-performance liquid chromatographic determination of carnosic acid and carnosol in *Rosmarinus officinalis* and *Salvia officinalis*. *J. Chromatogr. A* **1994**, 679, 381–386.

(15) Maxwell, R. J. Solubility Measurements of Lipid Constituents in Supercritical Fluids. *Supercritical Fluid Technology in Oil and Lipid Chemistry*; AOCS Press: Champaign, IL, 1996.

(16) Olszewska, M. Optimization and Validation of an HPLC–UV Method for Analysis of Corosolic, Oleanolic, and Ursolic Acids in Plant Material: Application to *Prunus serotina* Ehrh. *Acta Chromatogr.* **2008**, 20, 643–659.

(17) Kumoro, A. C.; Singh, H.; Hasan, M. A. Solubility of piperine in supercritical and near critical carbon dioxide. *Chin. J. Chem. Eng.* **2009**, 17, 1014–1020.

(18) Catchpole, O. J.; von Kamp, J. C. Phase equilibrium for the extraction of squalene from shark liver oil using supercritical carbon dioxide. *Ind. Eng. Chem. Res.* **1997**, 36, 3762–3768.

(19) *Thermophysical Properties of Fluid System*; National Institute of Standards and Technology: Gaithersburg, MD. Available online: <http://webbook.nist.gov/chemistry/fluid> (accessed Oct 2010).

(20) Garmroodi, A.; Hassan, J.; Yamini, Y. Solubilities of the drugs benzocaine, metronidazole benzoate, and naproxen in supercritical carbon dioxide. *J. Chem. Eng. Data* **2004**, 49, 709–712.

(21) Chimowitz, E. H.; Kelley, F. D.; Munoz, F. M. Analysis of retrograde behavior and the crossover effect in supercritical fluids. *Fluid Phase Equilib.* **1988**, 44, 23–52.

(22) Murga, R.; Sanz, M. T.; Beltrán, S.; Cabezas, J. L. Solubility of syringic and vanillic acids in supercritical carbon dioxide. *J. Chem. Eng. Data* **2004**, 49, 779–782.

(23) Sparks, D. L.; Hernandez, R.; Estévez, L. A.; Meyer, N.; French, T. Solubility of Azelaic Acid in Supercritical Carbon Dioxide. *J. Chem. Eng. Data* **2007**, 52, 1246–1249.

(24) Chrastil, J. Solubility of Solids and Liquids in Supercritical Gases. *J. Phys. Chem.* **1982**, 86, 3016–3021.

(25) Brennecke, J. F.; Eckert, C. A. Phase equilibria for supercritical fluid process design. *AIChE J.* **1989**, 35, 1409–1427.

(26) Adachi, Y.; Lu, B. C. Y. Supercritical fluid extraction with carbon dioxide and ethylene. *Fluid Phase Equilib.* **1983**, 14, 147–156.

(27) del Valle, J. M.; Aguilera, J. M. An improved equation for predicting the solubility of vegetable oils in supercritical CO₂. *Ind. Eng. Chem. Res.* **1988**, 27, 1551–1553.

(28) Lyman, W. J.; Reehl, W. F.; Rosenblatt, D. H. *Handbook of Chemical Property Estimation Methods*; American Chemical Society: Washington, DC, 1990.

(29) Méndez-Santiago, J.; Teja, A. S. The solubility of solids in supercritical fluids. *Fluid Phase Equilib.* **1999**, 158, 501–510.